Taylor & Francis
Taylor & Francis Group

Experimental Heat Transfer

A Journal of Thermal Energy Generation, Transport, Storage, and Conversion

ISSN: 0891-6152 (Print) 1521-0480 (Online) Journal homepage: https://www.tandfonline.com/loi/ueht20

Experimental investigation of the thermal performance of closed loop flat plate oscillating heat pipe

Kamlesh Mehta, Nirvesh Mehta & Vivek Patel

To cite this article: Kamlesh Mehta, Nirvesh Mehta & Vivek Patel (2020): Experimental investigation of the thermal performance of closed loop flat plate oscillating heat pipe, Experimental Heat Transfer, DOI: 10.1080/08916152.2020.1718802

To link to this article: https://doi.org/10.1080/08916152.2020.1718802

Published online: 23 Jan 2020.

EXPERIMENTAL HEAT TRANSFER
https://doi.org/10.1080/08916152.2020.1718802

Experimental investigation of the thermal performance of closed loop flat plate oscillating heat pipe

Kamlesh Mehta [a], Nirvesh Mehta [b], and Vivek Patel [c,d]

[a]Department of Mechanical Engineering, Gujarat Technological University, Ahmedabad, Gujarat, India; [b]Department of Mechanical Engineering, Government Engineering College, Dahod, Gujarat, India; [c]Department of Mechanical Engineering, Pandit Deendayal Petroleum University, Gandhinagar, India; [d]The Shaanxi Key Laboratory of Friction Welding Technologies, Northwestern Polytechnical University, Shaanxi, China

ABSTRACT

A number of theoretical studies and experimental investigations have been carried out on the closed loop flat plate oscillating heat pipe (CLFP-OHP) in the past decades. However, due to the complex working mechanism of CLFP-OHP, the effects of operational and geometrical parameters on the thermal performance CLFP-OHP have not been completely revealed so far. In the present study, the CLFP-OHP was investigated with different operational parameters (charge ratio, orientation, and heat load) and geometrical parameters (channel size and shape). In order to investigate the effect of these parameters, parallel mini channels were machined onto the copper plate and acetone was used as working fluid to form CLFP-OHP. An attempt has been made to resolve the critical charge ratio of acetone for CLFP-OHP. The measured thermal resistance found strongly dependent on operational and geometrical parameters. The best performance was observed by acetone with a charge ratio of 60% in the vertical orientation for square (2 x 2 mm^2) channels. The lowest thermal resistance of 0.39°C/W achieved for acetone at 100 W. The thermal conductivity of CLFP-OHP reached to 3205 W/m °C.

ARTICLE HISTORY
Received 3 September 2019
Accepted 16 January 2020

KEYWORDS
Flat plate oscillating heat pipe; Oscillation motion; Thermal resistance; Heat transfer

Introduction

Heat pipes are used in various systems due to their effective thermal management capacity [1, 2]. As the heat dissipation rate continues to increase in new upcoming systems, the focus shifted to new heat transfer devices [3–9]. The thermal management challenges were not limited to electronics industries, similar challenges began to emerge in different components found in various engineering systems [10, 11]. The conventional heat pipe cannot always give effective thermal management due to limitations on miniaturizing of systems [12–15]. The oscillating heat pipe (OHP) was invented by Akachi [16]. Since then oscillating heat pipe was considered to have great application possibilities in the area of waste heat recovery, solar energy utilization and aerospace industries due to its several advantages like simple construction, miniaturization, high heat transfer capacity, flexibility and low cost [13, 14, 17]. Generally, oscillating heat pipe exists as a capillary tube bent in many turns, namely tubular oscillating heat pipe (T-OHP) as shown in Figure 1(a) and flat plate oscillating heat pipe 1(b) (FP-OHP) [18, 19]. FP-OHP is developed to solve some shortcomings of the tubular oscillating heat pipe (i.e. low heat dissipation, less feasible for electronics system, etc.) [20–25]. FP-OHP consists of parallel mini channels manufactured in a metal plate as shown in Figure 1(b).

FP-OHP is a reliable, simple, and economical choice for effective heat transfer. FP-OHPs are available in three forms of open loop, closed loop and closed loop with check valves. The closed loop flat plate oscillating heat pipe (CLFP-OHP) is more suitable because of its ability to generate stronger

CONTACT Kamlesh Mehta kamleshnit1@yahoo.com Department of Mechanical Engineering, Gujarat Technological University, Ahmedabad, Gujarat 382424, India

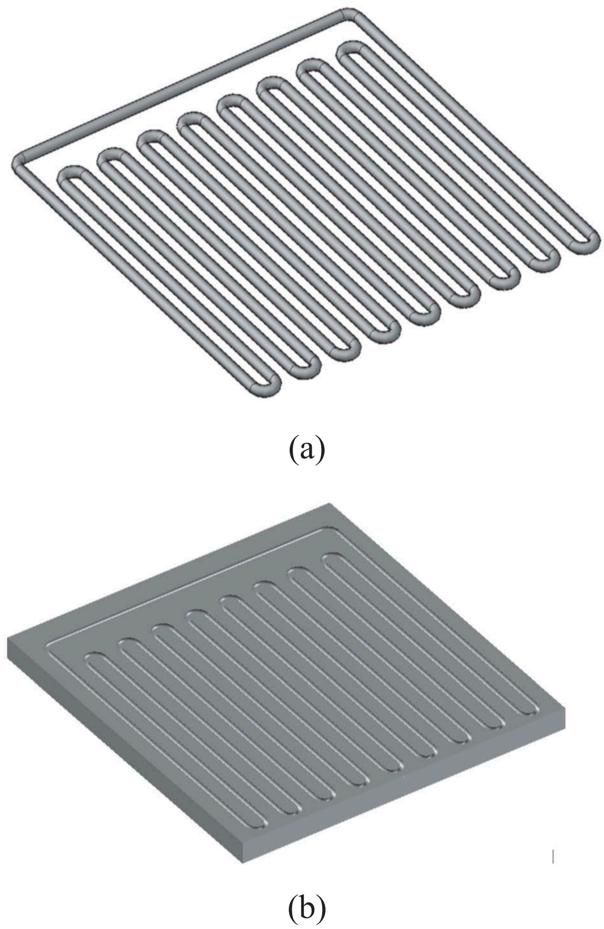

Figure 1. (a) A tubular oscillation heat pipe (T-OHP) (b) A flat plate oscillating heat pipe (FP-OHP).

oscillation motion of liquid slugs and vapor bubbles [26]. The CLFP-OHP consists of evaporator, condenser and adiabatic sections as shown in Figure 2. The working fluid is partially charged in CLFP-OHP, and heat load is applied to the evaporator section. This results in the growth of vapor plugs in the evaporator section. Enlarged vapor plugs push the liquid slugs toward the condenser section. The condenser section cools down the vapor plugs, and vapor pressure reduces. The growth and contraction of vapor plugs result in an oscillatory flow of liquid slugs and vapor plugs in CLFP-OHP. The heat transfer is a kind of sensible heat form within liquid slugs and latent heat form in vapor plugs [27–30]. Due to the high vapor pressure generated in the evaporator section, the vapor plug pushes the liquid slug toward the condenser section. The adiabatic section acts as an insulated channel to transport liquid slugs and vapor plugs between evaporator and condenser sections.

In the past few years, several theoretical and experimental studies have been conducted on the heat transfer characteristics of CLFP-OHP, which identified the oscillation motion of liquid slugs and vapor plugs during operation. Stevens et al. [31] identified that the orientation, configuration and heat load all influenced the level of variation in the thermal performance of CLFP-OHP. It can be studied that the effect of various parameters is very complicated due to the coupling of the hydrodynamic and thermodynamic influence in CLFP-OHP.

In order to study the experimental investigations of the CLFP-OHP more clearly, the operational and geometrical data of previous research are summarized in Table 1 [23, 32–37, 39–48]. Previous researches have investigated the thermal performance of CLFP-OHP with different working fluids and specific charge

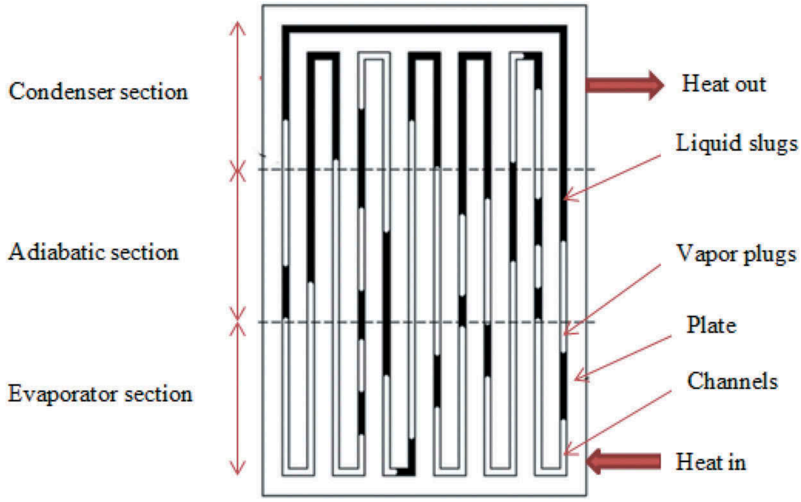

Figure 2. Closed loop flat plate oscillating heat pipe working.

ratios. Due to the lack of complete understanding, results of experiments and numerical simulations still have contradictions [49]. Till date there is no best model of CLFP-OHP which can give the optimum thermal performance over a wide range of operations. As a result, CLFP-OHP has not been commercially used in a wide range. The above literature survey shows that the effects of various parameters on the thermal performance of CLFP-OHP are limited. Further, most of the experimental studies have been done with specific operational and geometrical parameters. This provides only a partial picture of the complex working mechanism in CLFP-OHP. There could be no doubt that effects of operational and geometrical parameters are essential for a proper assessment of the thermal performance of CLFP-OHP. This has been the motivation of the present research. Researchers [13, 17, 33, 50–55] divided parameters into three categories: (1) operational parameters: charge ratio; orientation; heat load, (2) geometrical parameters: channel size; channel shape; number of channels, and (3) working fluid. Accordingly, a series of experiments have been conducted to know these effects on CLFP-OHP at different heat loads.

Experimental methods

Development of flat plate oscillating heat pipe (CLFP-OHP)

The CLFP-OHP test section was made of copper with 18 parallel mini channels machined by the vertical milling machine. The details of the CLFP-OHP test section are shown in Figure 3. The hydraulic radius of the channel must be small enough such that surface tension forces dominate compared to gravitational force and a distinct formation of liquid slugs and vapor plugs is able to form in the CLFP-OHP [18, 21]. The maximum radius of the channel in CLFP-OHP is given by the Bond number as follows [56]:

$$\mathrm{Bo} = \frac{g(\rho_l - \rho_v) r_{h,max}^{\ 2}}{\sigma} \tag{1}$$

Where g,ρ_l, ρ_v, and σ are the gravitational force, liquid density, vapor density, and surface tension respectively. The Bond number is the ratio of the surface tension to the body force. Rearranging Eq. (1), the maximum hydraulic radius of the channel for CLFP-OHP can be found as:

$$r_h, \max \leq \sqrt{\frac{\sigma \mathrm{Bo}}{g(\rho l - \rho v)}} \tag{2}$$

Table 1. The operational and geometrical data of previous researches.

Investigators	Working Fluid	Evaporator Size (mm^2)	Condenser Size (mm^2)	Number of Channel	Size of Channel (mm^2)	Heat Load (watt)	Charge Ratio
Khandekar et al. [32]	Water	30 × 22	30 × 13	12	2.2 × 2	25–70	25%
	Ethanol						30%
							70%
Yang et al. [33]	Ethanol	100 × 30	100 × 60	40	2 × 2	10–200	90%
Qu et al. [34]	Acetone	20 × 60	100 × 60	22	1.5 × 1.5	10–100	50%
							20.90%
Chang et al. [35]	Acetone	25.4 × 25.4	25.4 × 90	16	0.762 × 0.762	10–140	70%
	Water			10	1 × 1		
	Nano fluids			8	1.7 × 1.175		
					1.75 × 1.17		
Thompson et al. [23]	Acetone	63.5 × 31.75	76.2 × 76.2	15	0.762 × 0.762	10–180	73%
Chien et al. [36]	Distilled water	15 × 40	40 × 40	8	2 × 2	140	40%
							50%
							60%
							70%
Lefevre et al. [37]	Methanol	190 × 90	30 × 90	8	4 × 4	80	70%
	FC-72						
Hoesing et al. [38]	Water	83 × 32	82.5 × 31.75	10	2 × 2	10–100	75%
Laun et al. [39]	Acetone	80 × 30	15 × 30	20	1.3 × 1.3	50–500 W	80%
Hao et al. [40]	De-Ionized Water	57 × 28	57 × 36	6	2 × 2	50–80	55%
Thompson et al. [41]	Acetone	30 × 30	30 × 30	15	1.02 × 1.02	50–250 W	80%
Manno et al. [42]	Ethanol	105 × 45	125 × 67	10	2 × 2	10–100	50%
Ayel et al. [43]	FC-72	10 × 120	200 × 120	12	1.6 × 1.7	30 − 180	50%
Zhang et al. [44]	HPLC water	25 × 40	30 × 40	10	1 × 1.5	75–225	65%
Lee et al. [45]	FC-72	10 × 16	15 × 16	5	2 × 2	50	50%
Jang et al. [46]	FC-72	25 × 54	25 × 54	5	2 × 2	5–28	70%
Yoon et al. [47]	Ethanol	10 × 18	18 × 18	5	1 × 0.5	5–20	55%

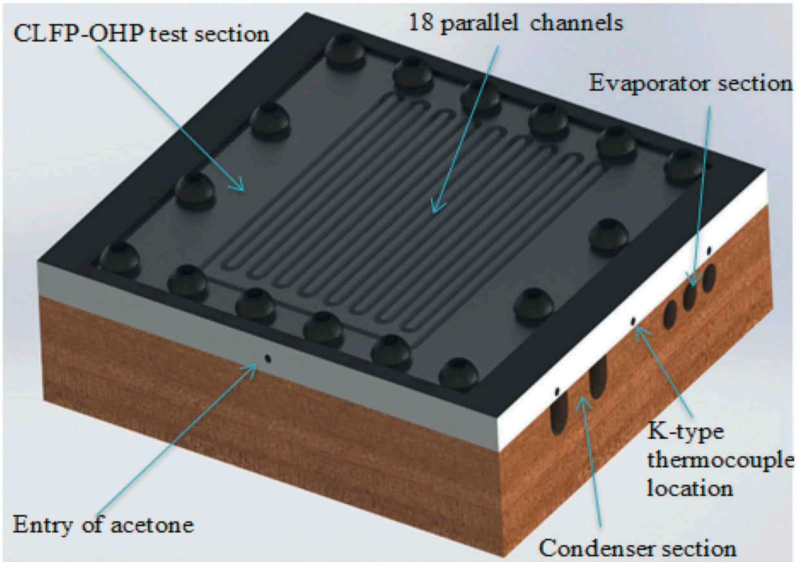

Figure 3. Details of CLFP-OHP test section.

Table 2. Properties of acetone at 25°C and 1 atm.

Property	Acetone
Boiling point (°C)	56
Surface tension (N/m) $\times 10^{-3}$	22.98
Liquid density (Kg/m^3)	784.5
Vapor density	0.74
Liquid specific heat (KJ/Kg°C)	2.33
Dynamic viscosity (Pa-sec)$\times 10^{-3}$	0.31

Akachi et al. suggested the Bond number should be equal to 1. It is widely reported that if Bo≤1, the effect of the surface tension force of working fluid dominates over that of gravitational force [57–59]. The thermophysical properties of acetone are tabulated in Table 2 using Engineering Equation Solver software [18].

The bond number value is highly debatable and further investigation needs to be done to determine its value for various fluids. This investigation used a Bo of 1, as reported in the previous study [31, 49, 57, 60–69].

To investigate the effect of operational parameters on CLFP-OHP square 2 × 2 mm^2 channel was used in the current study. The hydraulic radius of 2 × 2 mm^2 square channel is within range of calculated r_h, max. Hao et al. [40, 59] found that start time of CLFP-OHP is increased by using the hydrophilic surface. The test section plate was surface treated by using sulfuric acid after fabrication. An acrylic plate of 3 mm thickness was fabricated to seal the square channels, and fastened to the copper plate using a gasket. The evaporator section, condenser section, and adiabatic section was 30 × 70 mm^2 respectively as shown in Figure 4. Copper charge tube was brazed to charge the acetone in the CLFP-OHP as shown in Figure 5.

Experimental apparatus

The experimental setup is shown in Figure 6. Based on the literature review, a similar experimental methodology [67, 70] is chosen. It consists of a CLFP-OHP, temperature scanner, USB 485 coveter,

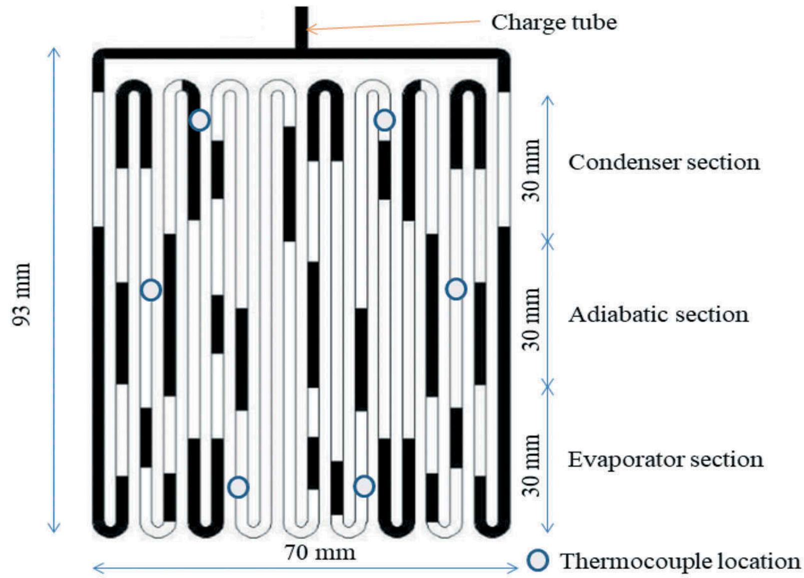

Figure 4. Schematic of CLFP-OHP.

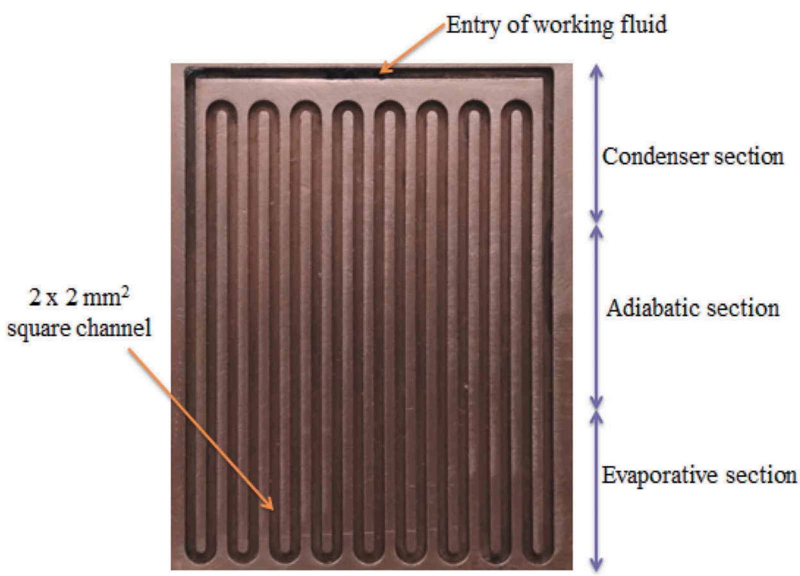

Figure 5. Photograph of CLFP-OHP.

laptop, heat load input system, water supply, and stand. The evaporator and condenser sections were developed from the copper blocks size of 30mm × 70mm × 10mm via milling machine. The slots are created on the copper heating block to house the 3 cartridge heaters in the bakelite board. Each cartridge heater contains a capacity of 100 W. The evaporator section was heated by copper heating block. The condenser section was in direct contact with a copper cooling block which was cooled by a constant-temperature cooling source. The backsides of the evaporator and condenser sections were thermally insulated with a bakelite board to reduce the heat loss to the surrounding atmosphere. The Heat load input system is used to control heat load to the evaporator section by adjusting current and voltage to the

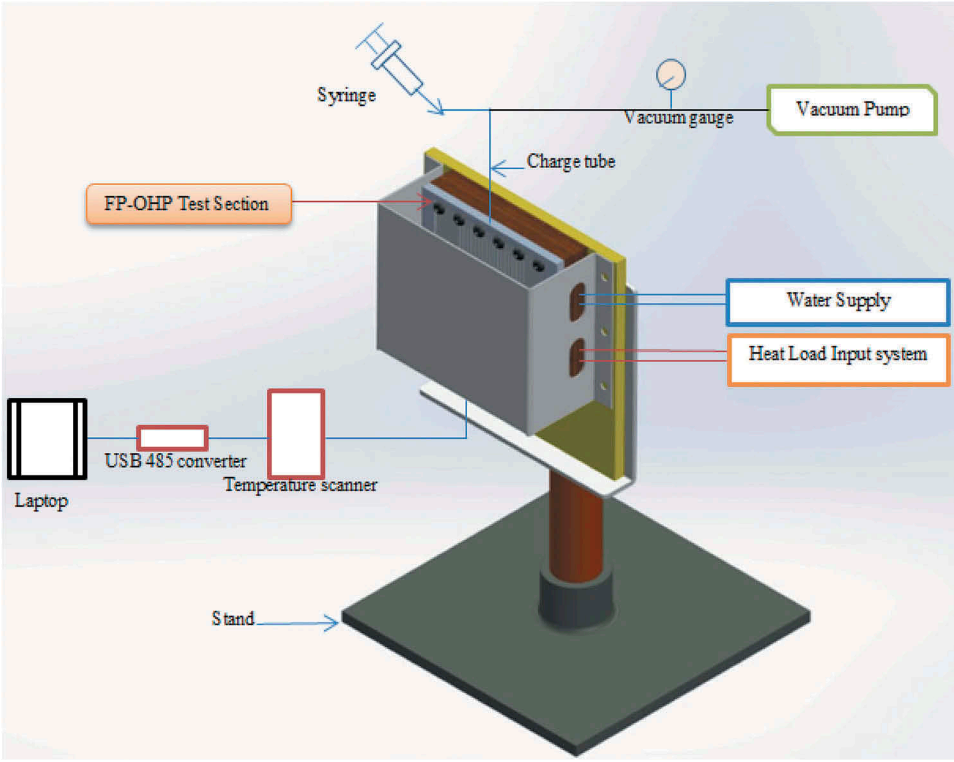

Figure 6. Experiment set up.

cartridge heaters. Total of six K-Type thermocouples of ± 0.5°C accuracy were used to measure temperature responses. Six thermocouples attached on both sides of CLFP-OHP to measure the temperature at various locations. The MASIBUS make data scanner used to record temperature data to the laptop through a USB 485 converter, as shown in Figure 7. The temperature data scanner has an accuracy of 0.1%. The temperature data logging to the laptop was interfaced through by MASIBUS software.

To charge the CLFP-OHP to a specified charge ratio, the test section was vacuumed to a pressure of 0.01mbar, by using a mechanical rotary vacuum pump. Then, a specified amount of working fluid charged into the CLFP-OHP by using a medical syringe. The heat load to the evaporator section was adjusted after the CLFP-OHP test section reached to steady state condition. A constant heat load was applied to the evaporator section via copper heating block and the condenser section was cooled via copper water cooling block with the inlet water temperature at 25°C (±0.1°C). The temperature measurements were recorded for heat load ranging from 10 W to 150 W in the step of 10 W. After confirming the constant temperature of all the K-Type thermocouples mounted in the CLFP-OHP test section, the heat load input system switched on and desire heat load was applied through the variable transformer. The experiment procedure was repeated for all parameters.

Uncertainty analysis

The thermal performance of CLFP-OHP on basis of thermal resistance is calculated from the Eq. (3).

$$R_{th} = \frac{T_e - T_c}{Q} \tag{3}$$

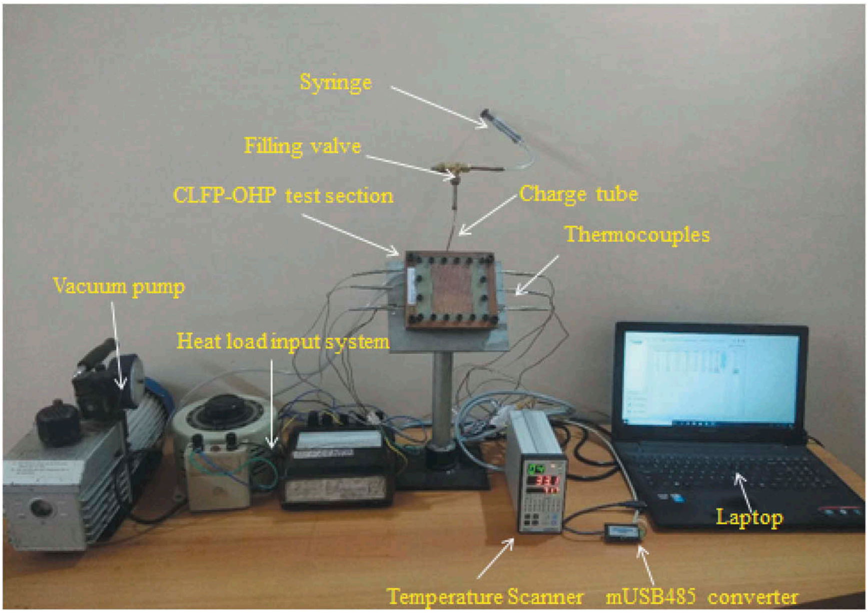

Figure 7. Experimental apparatus.

Where, T_e, T_c, and Q are the average temperatures of the evaporator, condenser, and heat load, respectively. The uncertainty analysis of CLFP-OHP is as follows [71]:

$$Q = U \times I \tag{4}$$

The uncertainties can be expressed:

$$\frac{\partial Q}{Q} = \sqrt{\left(\frac{dU}{U}\right)^2 + \left(\frac{dI}{I}\right)^2} \tag{5}$$

$$\frac{\partial R}{R} = \sqrt{\left(\frac{\delta T_e}{T_e - T_c}\right)^2 + \left(\frac{\delta T_c}{T_e - T_c}\right)^2 + \left(\frac{\delta Q}{Q}\right)^2} \tag{6}$$

The voltage and current of the heat load input system have accuracies both of 0.5. For 10 W, the detailed measured data are: U = 30 V, I = 0.33 A, T_e-T_c = 13°C (Acetone, charge ratio = 60%); then

$$\frac{\partial Q}{Q} = \sqrt{\left(\frac{0.5\% \times 80}{30}\right)^2 + \left(\frac{0.5\% \times \ 1}{0.3}\right)^2} = 2.31\% \tag{7}$$

$$\frac{\partial R}{R} = \sqrt{\left(\frac{0.5}{13}\right)^2 + \left(\frac{0.5}{13}\right)^2 + (2.13)^2} \tag{8}$$

Selected coverage factor (K) as 2, then maximum uncertainty (U_{max}) is:

$$U_{max} = K \times \frac{\partial R}{R} = 2.13\% \times 2 = 4.26\% \tag{9}$$

This is the maximum one for its small heat load and small temperature difference.

Results and discussion

Effect of operational parameters

In CLFP-OHP, the thermal performance is significantly affected by the oscillation motion of the working fluid. According to flow observation of CLFP-OHPs by Yoon et al [72], the flow characteristics in CLFP-OHPs strongly depend on the operational parameters. To figure out how the different operational parameters affect the thermal performance of CLFP-OHP, the experimental results are presented.

Effect of charge ratio

The effect of different charge ratio on the thermal performance of CLFP-OHP is analyzed. The charge ratio is defined as the ratio of working fluid volume to the total volume of the CLFP-OHP. The oscillating motion of liquid slugs and vapor plugs in CLFP-OHP depends on the charge ratio. At 100% charge ratio, the CLFP-OHP works as a single phase thermosyphon. Also, at 0% charge ratio, CLFP-OHP works as a conduction mode of heat transfer with high thermal resistance. After calibrating equipment, the experiments were conducted to know the effect of charge ratio of acetone on the thermal performance of CLFP-OHP at a given heat load. The CLFP-OHP was charged with different charge ratios from 20% to 70% in steps of 10% in the vertical orientation. Experimental studies have shown that when the charge ratio is between 20% and 80%, the CLFP-OHP can operate normally [22, 31–46]. Typical charge ratios reported in the literature for water, methanol, ethanol are between 50% and 70% [17, 21, 31, 66]. In present work, an attempt has been made to resolve the critical charge ratio of acetone for CLFP-OHP. The CLFP-OHP failed to start-up when it was charged at the lowest charge ratio up to 30%. The phenomenon of dry-out was observed in CLFP-OHP for 20% and 30%.

The flow visualization was captured by a video camera in CLFP-OHP channels as shown in Figure 8. According to the flow visualization study, the dry-out phenomena was observed at 20% and 30% charge ratio due to the shortage of liquid supply on the inner wall of the evaporator section. Therefore, acetone cannot develop the oscillation motion in CLFP-OHP at 20% and 30% charge ratios as shown in Figure 8(a). Also, weak oscillation motion was observed due to insufficient evaporation for the driving force, which results in the degradation of the thermal performance of the CLFP-OHP (Figure 8(b)). It is found that the stronger oscillation motion of liquid slugs and vapor plugs in the CLFP-OHP at 60% charge ratio (Figure 8(c)) within the evaporator region could be approximately divided into two sections of interest, namely the large oscillation region and small oscillation region. Different flow patterns, including slug flow, injection flow, and semi-annular /annular flow, were observed in this CLFP-OHP. Normally, the flow pattern has a significant influence on the CLFP-OHP performance.

Sun et al. observed that compared to the slug flow, semi-annular/annular flow is related to higher thermal performance [73]. At the charge ratio of 60%, more channels at the evaporator section were occupied by semi annular/annular flow as compared to charge ratios of 40% and therefore contributed to higher thermal performance as evidence in Figure 9. It can be seen from Figure 9, the CLFP-OHP with a charge ratio of 40% does not decrease the thermal resistance after 90 W as compared to the other charge ratio. These results indicate a poor performance at 40% charge ratio after 90 W. This is due to the fact that there are too many vapor plugs in the channels and it is very hard to maintain the stable oscillation. The oscillation motion of liquid slugs and vapor plugs in channels is mainly driven by the pressure variation occurring within the CLFP-OHP during the sensible and latent heat transport. Oscillation motion in channels is related to charge ratio and it is found to be increasing with the increase in charge ratio [49]. It reveals that enough charge ratio is

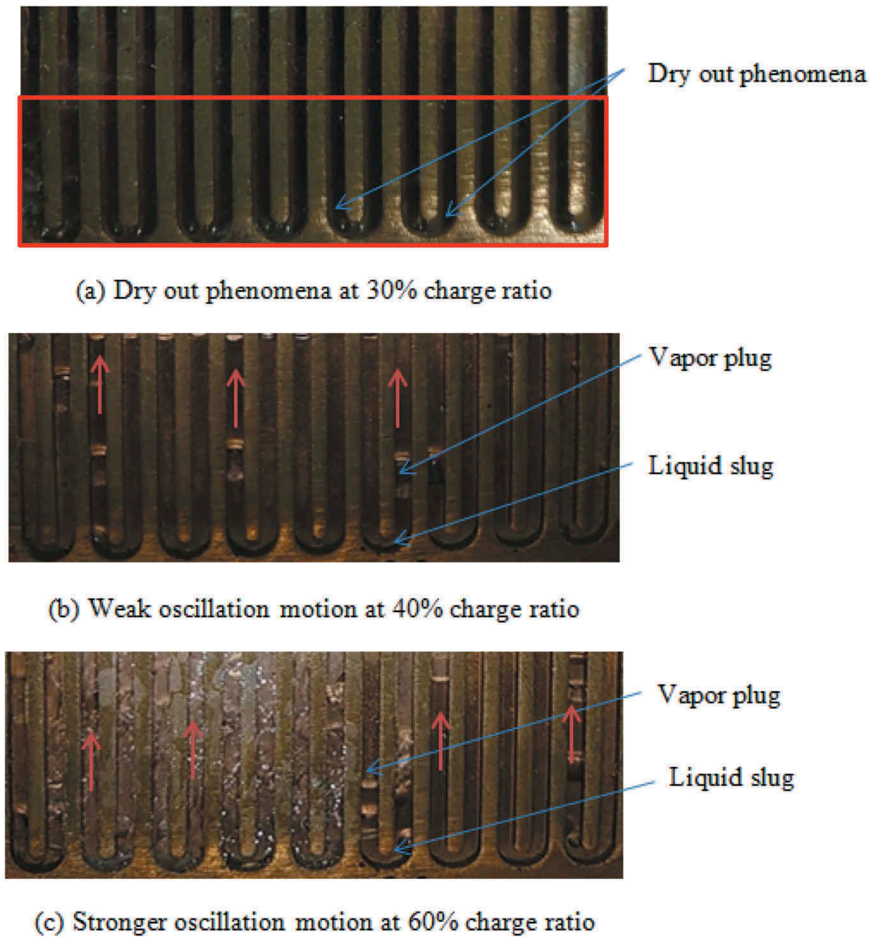

Figure 8. Effect of charge ratio on the internal flow patterns inside the CLFP-OHP.

required to sustain the oscillation motion in CLFP-OHP. It was found that CLFP-OHP is working when the charge ratio above 50%. The best thermal performance was observed for 60% charge ratio at 100 W heat loads. The lowest thermal resistance of 0.39°C/W is achieved for 60% charge ratio. The 70% charge ratio gives better performance as compared to other charge ratios, except 60% charge ratio. The reason for the degradation of performance of CLFP-OHP at 70% charge ratio is few vapor plugs in the channels, causing a decrease in the driving force of the working fluid. Hence, the oscillation motion is reduced as compared to 60% charge ratio.

Effect of orientation

From the literature survey, it can be understood that if the hydraulic radius of the channel satisfies Eq. (3), the impact of surface tension will be stronger than gravity. Qu et al. [55] found that gravity has a significant influence on the thermal performance of CLFP-OHP. The methods utilized to know the effect of the gravity can be classified into two groups, one by changing the orientation of the CLFP-OHP and other is by changing the gravity field [17]. The heat transfer performance of CLFP-OHP is very noticeable when the orientation is changed from a vertical orientation (90°). Vassilev et al. [74] found that the thermal performance of the CLFP-OHP changed with the orientation when

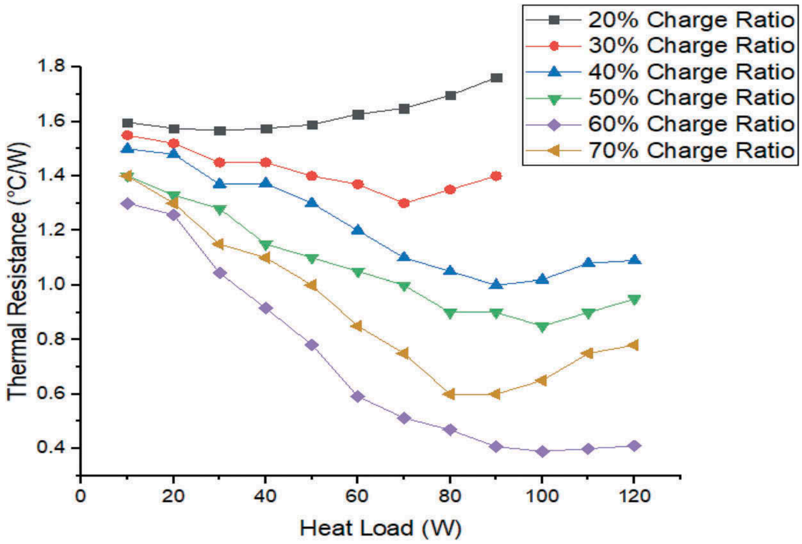

Figure 9. Thermal resistance of CLFP-OHP at different charge ratio.

it was within the range of vertical (90°) to horizontal(0°) orientation. In this investigation, four orientations were tested from vertical (90°) to horizontal (0°) in steps of (30°).

The charge ratio of 60% is used in this study, which has lower thermal resistance as compared to other charge ratios. Experimental results exhibited better performance in the vertical orientation as shown in Figure 10. In the vertical orientation, the liquid slugs and vapor plugs oscillated more during operation and resulted in a stronger oscillation motion of acetone in CLFP-OHP. At 100 W heat loads, the thermal resistance of vertical orientation (90°) was 35% lower than the 60° orientation and 62% lower than the 30° orientation. It can be seen that for orientation other than the vertical, the

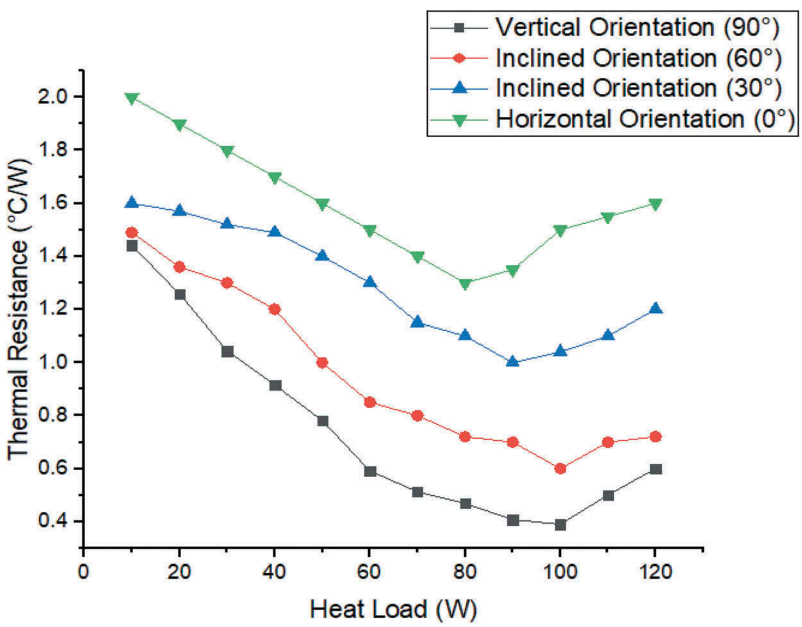

Figure 10. Thermal resistance of CLFP-OHP at different orientation.

thermal resistance is always higher, indicating a case of less oscillation motion of liquid slugs and vapor plugs in CLFP-OHP. It is clear that gravity has a role to play in the oscillation motion of working fluid in channels. Gravity also enables the condensed working fluid in the channels to flow back to the evaporator section for oscillation motion without the use of external force. So, it was observed that vertical orientation gives better performance as compared to other orientation.

The thermal performance of CLFP-OHP can be varying when the working conditions are different from charge ratios and heat loads. An attempt has been made to know the effect of charge ratio with varying orientation for 100 W. The CLFP-OHP was tested with charge ratios 40% to 70% in steps of 10%, with orientations changed starting from vertical orientation (90°) in the sequence of 90°-60°-30°-0°. For each orientation 20 min was allowed to achieve steady-state condition before moving over to the new orientation. From Figure 11 it can be inferred that the thermal resistance of 60% charge ratio was the most favorable across all the orientations. The thermal resistance of 50% charge ratio was found to be more suitable at lower orientations than 40 and 70% charge ratio. The 40% charge ratio was even lesser in terms of thermal performance compared to other charge ratios. The 70% charge ratio was less effective in performance as compared to the 60% charge ratio. This is due to the less oscillation motion of working fluid that reduces performance.

Effect of geometrical parameters

The purpose of the present investigation is to know the effect of geometrical parameters on the thermal performance of CLFP-OHP. For this purpose, CLFP-OHP with a square cross-section of 5×5 mm^2 and circular cross-section were fabricated. The size of the evaporator and condenser sections is kept the same for this investigation.

Effect of channel size

It has been studied that many geometrical parameters can affect the thermal resistance of CLFP-OHP. However, the thermal resistance of CLFP-OHP was not investigated in detail for channel sizes. The optimum conditions of CLFP-OHP parameters tend to vary accordingly to channel size [18, 68]. The objective of this investigation is to understand the influence of channel size on the thermal resistance of CLFP-OHP with square cross-section of 2×2 mm^2 and 5×5 mm^2. The influence of

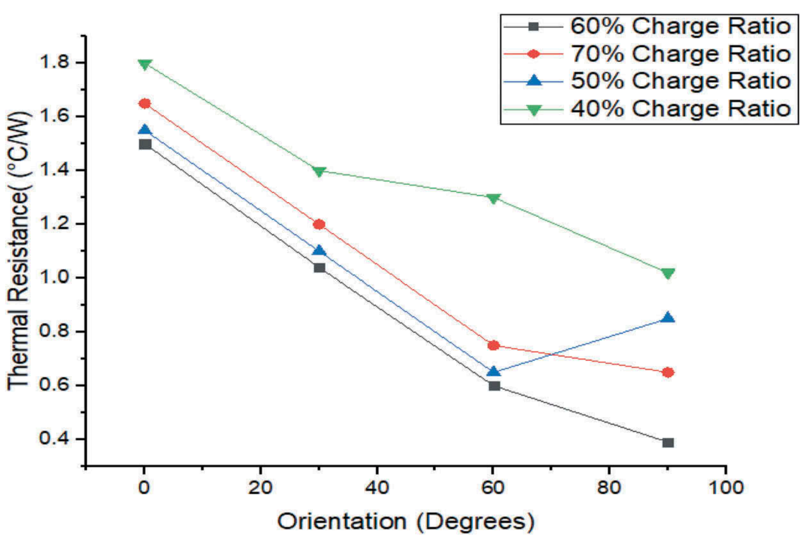

Figure 11. Effect of charge ratio with varying orientation.

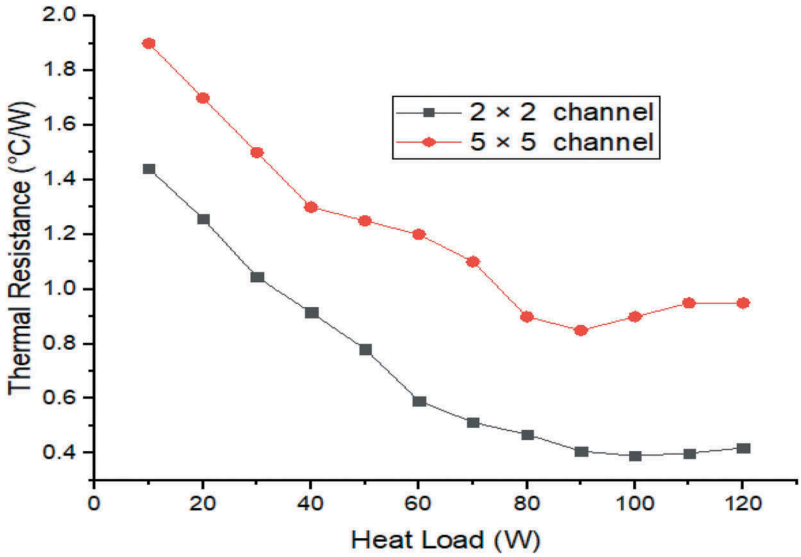

Figure 12. Effect of channel size.

channel size on the thermal resistance of CLFP-OHP is shown in Figure 12. The result indicates that the lower thermal resistance of 0.39°C/W is achieved with a square 2 × 2 mm^2 channels. This is due to the stronger surface tension force at the reduced channel size in CLFP-OHP. The thermal performance of 5 × 5 mm^2 channels showed poor performance at the heat load of 100 W because the pressure fluctuation at evaporator and condenser sections became small with the flow types change from more oscillation to less oscillation of liquid slugs and vapor plugs. At the 5 × 5 mm^2 square channels, the heat transfer is decreased as compared to 2 × 2 mm^2 square channels due to insufficient startup heat load with 5 × 5 mm^2 square channels. At the heat load of 10 W, oscillation motion occurred relatively early with 2 × 2 mm^2 square channel sizes. The thermal performance was the highest at the 2 × 2 mm^2 square channels due to the increased oscillation motion and decreased working fluid resistance. To start the two-phase flow in CLFP-OHP, the motion suffers due to working fluid resistance. Also, it is observed from Table 1 [22, 31–46] that the smaller channel size is more favorable to CLFP-OHP to get effective heat transfer. It is noted that the two-phase heat transfer plays an important role to enhance thermal performance in CLFP-OHPs attributed to small channel sizes.

Effect of channel shape

The effect of different channel shapes on the thermal resistance of CLFP-OHP is analyzed. The oscillating motion of working fluid in CLFP-OHP depends on the channel shapes. To understand the effect of channel shape, the hydraulic radiuses of square and circular shape are kept same. Figure 13 represents the effect of the square and circular shapes on the thermal resistance of CLFP-OHP. With the heat load of 100 W, the lowest thermal resistance of CLFP-OHP was achieved to be 0.39°C/W. The square channel CLFP-OHP obtained up to 35% lower thermal performance in terms of thermal resistance than the circular channel. Khandekar et al. [32] recommended that the thermal resistances are typically lower for square channels compared to circular channels having the same hydraulic radius. It is observed that the square channel CLFP-OHP can manage lower thermal resistance than the circular channel CLFP-OHP. This is due to the fact that the square channel shapes allowed the working fluid to pass along the channels. Initially, a weak oscillation of working fluid occurred in square and circular channels with low range of the heat load at the evaporator section.

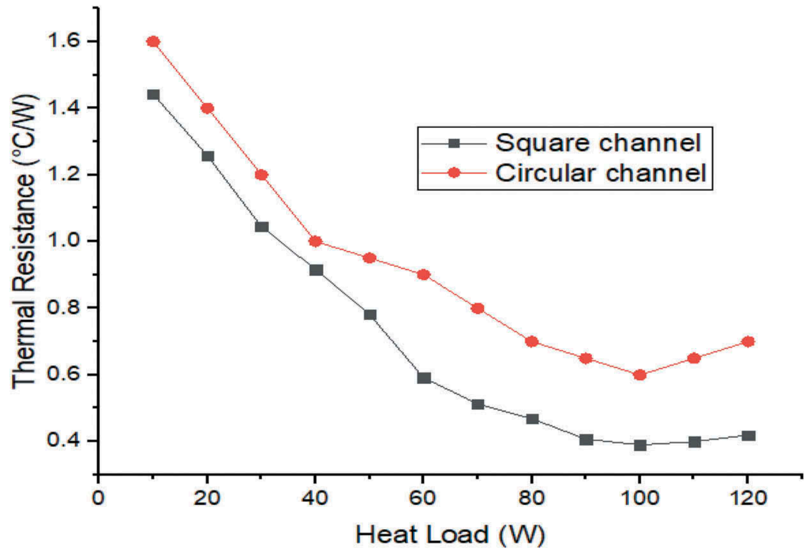

Figure 13. Effect of channel shape.

As the heat load increases further in the CLFP-OHP with square channels, the oscillation motion of working fluid occurs in a wide region, which enhances the heat transfer. As compared to circular channels, square channels oscillation motion occurs easily, as liquid slugs and vapor plugs move through square channels. The pressure difference at the evaporator section and condenser section helps to oscillate the acetone through small channels, which can enhance the motion of working fluid. In square channels, the amount of liquid slugs and vapor plugs flow increases with increasing the heat loads. The increased amount of liquid slugs and vapor plugs leads to an increase in the oscillation motion, reducing the thermal resistance of the CLFP-OHP in comparison with circular channels. For the heat load above 50 W, the effect of channel shapes on the thermal resistance of CLFP-OHP became more substantial. It is postulated that when the working fluid charged in square channel CLFP-OHP, the two-phase heat transfer is much higher than for the equivalent CLFP-OHPs circular channel. It is noted that the CLFP-OHP with square channel shape has an advantage in terms of oscillation motion of working fluid over the circular channel shape.

Thermal conductivity of CLFP-OHP

A new thermal performance indicator, CLFP-OHP thermal conductivity is used in the assessment of the thermal performance of the device. The thermal conductivity is defined as:

$$k = \frac{Q}{Te - Tc}\frac{L}{A} \tag{9}$$

Where Q is the heat load, T_e and T_c are average temperatures of evaporator and condenser respectively, L is the distance of evaporator section and condenser section, and A is the total cross-sectional area of the CLFP-OHP. Figure 14 shows thermal conductivity based on Eq. 9 for CLFP-OHP. The thermal conductivity of CLFP-OHP increases with the increasing heat loads at the heat source section.

The reason is that the heat load is proportional to the thermal conductivity of the CLFP-OHP. It is noticed that the thermal conductivity increases with decreasing temperature difference of the evaporator section and condenser section. The thermal resistance of CLFP-

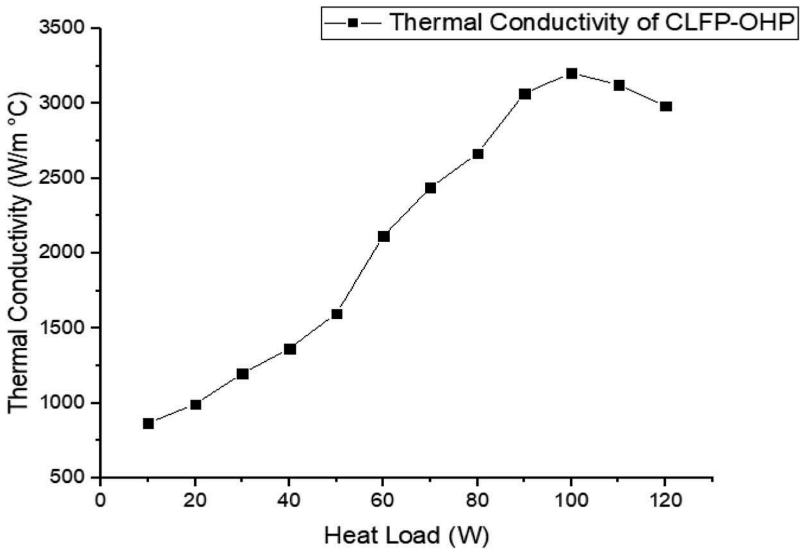

Figure 14. Thermal conductivity of CLFP-OHP.

OHP decreases with increasing the heat load, while the opposite trend found in the case of thermal conductivity. As shown in Figure 14, the thermal conductivity of CLFP-OHP is between 867 and 3205 W/m °C. For comparison, the thermal conductivity of CLFP-OHP is increased by a factor of 8.7% in comparison with that of pure copper (401 W/m °C). It is noted that the thermal conductivity of the CLFP-OHP is more than that of high purity copper, which is attributed to the oscillation motion of liquid slugs and vapor plugs in the CLFP-OHP between the evaporator and condenser sections.

Conclusion

The effects of the operational and geometrical parameters on the thermal performance of closed loop flat plate oscillating heat pipe (CLFP-OHP) were investigated with acetone as a working fluid. The series of experiments were carried out to find the influence of operational and geometrical parameters on the thermal resistance of CLFP-OHPs. The salient observations are as follows:

(1) The maximum performance was observed when the acetone was charged by 60%. The CLFP-OHP with a 60% charge ratio showed a stronger oscillation motion in comparison with that of other charge ratios.
(2) The oscillation motion of liquid slugs and vapor plugs determined the thermal performance of CLFP-OHP which improved with the vertical orientation (90°).
(3) The best channel shape and channel size of CLFP-OHP were square and 2×2 mm^2, respectively. The thermal performance of CLFP-OHP was significantly decreased in the 5×5 mm^2 channel size and circular channel. The surface tension forces of working fluid become much stronger as the channel size reduces.
(4) The lowest thermal resistance was achieved to be 0.39°C/W at 100 W. The flow pattern of liquid slugs and vapor plugs determined the thermal performance of CLFP-OHP which improved with the 2×2 mm^2 square channels.
(5) The thermal resistance of square 2×2 mm^2 CLFP-OHP was found to be lowest by 35% in comparison with that of circular channels.

(6) The thermal conductivity of CLFP-OHP was found to be highest by a factor of 8.7% in comparison with that of pure copper. Therefore, the CLFP-OHP has excellent heat transfer performance during the operation process, and it can remove the heat generation from various systems.

Nomenclature

Bo	Bond number, dimensionless
g	gravitational force, m/s^2
K	Thermal conductivity W/m°C
Q	Heat load, W
R_{th}	Thermal Resistance, °C/W
r	radius, mm
T	Temperature, °C

Greek Symbols

σ	density, kg/m^3
σ	Surface tension, kg/s^2

Subscripts

CLFP-OHP	closed loop flat plate oscillating heat pipe
c	condenser
e	evaporator
FP-OHP	flat plate oscillating heat pipe
h	hydraulic
l	liquid
v	vapor
T-OHP	tubular oscillating heat pipe

Funding

This project has been supported by the Gujarat Technological University [Grant No: 201921003211] under student startup and innovation Policy (SSIP).

ORCID

Kamlesh Mehta http://orcid.org/0000-0002-9602-4749

References

[1] D. J. Kearney, O. Suleman, J. Griffin, and G. Mavrakis "Thermal performance of a PCB embedded pulsating heat pipe for power electronics applications'" *Appl. Therm. Eng.*, vol. 98, pp. 798–809, April. 5. 2016. DOI: 10.1016/j.applthermaleng.2015.11.123.

[2] C. Dang, L. Jia, and Q. Lu "Investigation on thermal design of a rack with the pulsating heat pipe for cooling CPUs'" *Appl. Therm. Eng.*, vol. 110, pp. 390–398, January. 5. 2017. DOI: 10.1016/j.applthermaleng.2016.08.187.

[3] I. Mudawar "Recent advances in high-flux, two-phase thermal management'" *J. Therm. Sci. Eng. Appl.*, vol. 5, pp. 021012, May. 17. 2013. DOI: 10.1115/1.4023599.

[4] J. B. Marcinichen, J. A. Olivier, N. Lamaison, and J. R. Thome "Advances in electronics cooling'" *Heat Transfer Eng.*, vol. 34, pp. 434–446, Nov. 20. 2013. DOI: 10.1080/01457632.2012.721316.

[5] D. S. Naruka, R. Dwivedi, and P. K. Singh, "Experimental inquisition of heat pipe: performance evaluation for different fluids," *Exp. Heat Transfer*, pp. 1–15, 2020. DOI: 10.1080/08916152.2020.1713254.

[6] S. Caliskan, A. Dogan, and I. Kotcioglu. “Experimental investigation of heat transfer from different pin fin in a rectangular channel,” *Exp. Heat Transfer*, vol. 32, pp. 376–392, July. 04. 2019. DOI: 10.1080/08916152.2018.1526228.
[7] M. A. Alnakeeb, W. M. El-Maghlany, M. A. Teamah, and M. M. Sorour, “Experimental study of mixed convection from horizontal isothermal elliptic cylinders at different aspect ratios,” *Exp. Heat Transfer*, pp. 1–16, 2019. DOI: 10.1080/08916152.2019.1625468.
[8] X. Peng, D. Wang, G. Wang, Y. Yang, and S. Xiang, “Investigation of heat transfer performance and flow characteristic in helically coiled-twisted flat tube,” *Exp. Heat Transfer*, pp. 1–21, 2019. DOI: 10.1080/08916152.2019.1656300.
[9] C. K. Mangrulkar, *et al.*, “Thermal performance escalation of cross flow heat exchanger using in-line elliptical tubes,” *Exp. Heat Transfer*, pp. 1–26, 2019. DOI: 10.1080/08916152.2019.1704946.
[10] J. A. Olivier, J. B. Marcinichen, A. Bruch, and J. Thome “Green cooling of high performance microprocessors: parametric study between flow boiling and water cooling‘” *J. Therm. Sci. Eng. Appl.*, vol. 3, pp. 041003, Oct. 24. 2011. DOI: 10.1115/1.4004435.
[11] B. Agostini, *et al.* “State of the art of high heat flux cooling technologies‘” *Heat Transfer Eng.*, vol. 28, pp. 258–281, March. 6. 2007. DOI: 10.1080/01457630601117799.
[12] H. Yang, S. Khandekar, and M. Groll, “Performance characteristics of pulsating heat pipes as integral thermal spreaders,” *Int. J. Therm. Sci.*, vol. 48, pp. 815–824, 2009.
[13] S. Khandekar, M. Groll, P. Charoensawan, S. Rittidech, and P. Terdtoon, “Closed and open loop pulsating heat pipes,” Proceedings of 13th International Heat Pipe Conference, Shanghai,China, 2004.
[14] M. Groll and S. Khandekar, “Pulsating heat pipes: progress and prospects,” Proceedings of the International Conference on Energy and the Environment, China, 2003.
[15] S. Khandekar, N. Dollinger, and M. Groll, “Understanding operational regimes of closed loop pulsating heat pipes: an experimental study,” *Appl. Therm. Eng.*, vol. 23, pp. 707–719, 2003.
[16] H. Akachi, “Structure of a heat pipe,” USA Patent 4921041 A, 1990.
[17] X. Han, X. Wang, H. Zheng, X. Xu, and G. Chen, “Review of the development of pulsating heat pipe for heat dissipation,” *Renewable Sustainable Energy Rev.*, vol. 59, pp. 692–709, June. 2016. DOI: 10.1016/j.rser.2015.12.350.
[18] K. K. Mehta, N. Mehta, and V. Patel, “Effect of operational parameters on the thermal performance of flat plate oscillating heat pipe,” *J. Heat Transfer*, vol. 141, pp. 121802, 2019. DOI:10.1115/1.4044825.
[19] V. Patel, *et al.*, “Experimental Investigation of Flat Plate Cryogenic Oscillating Heat Pipe,” *J. Low Temp. Phys.*, vol. 198, pp. 41–55, 2019.
[20] X. Liu and Y. Chen, “Fluid flow and heat transfer in flat-plate oscillating heat pipe,” *Energy Build.*, vol. 75, pp. 29–42, June. 2014. DOI: 10.1016/j.enbuild.2014.01.041.
[21] Y. Zhang and A. Faghri “Advances and unsolved issues in pulsating heat pipes‘” *Heat Transfer Eng.*, vol. 29, pp. 20–44, Jul. 14. 2008. DOI: 10.1080/01457630701677114.
[22] B. Borgmeyer and H. Ma, “Experimental investigation of oscillating motions in a flat plate pulsating heat pipe,” *J. Thermophys Heat Transfer*, vol. 21, pp. 405–409, 2007. DOI:10.2514/1.23263.
[23] S. Thompson and H. Ma, “Effect of localized heating on three-dimensional flat-plate oscillating heat pipe,” *Adv. Mech. Eng.*, vol. 2, pp. 1–10, 2010. DOI:10.1155/2010/465153.
[24] L. Lv, J. Li, and G. Zhou, “A robust pulsating heat pipe cooler for integrated high power LED chips,” *Heat Mass Transfer*, vol. 53, pp. 3305–3313, 2017. DOI:10.1007/s00231-017-2050-3.
[25] N. Soponpongpipat, P. Sakulchangsatjaati, N. Kammuang-Lue, and P. Terdtoon, “Investigation of the startup condition of a closed-loop oscillating heat pipe,” *Heat Transfer Eng.*, vol. 30, pp. 626–642, 2009. DOI:10.1080/01457630802656876.
[26] J. Xu, Y. Li, and T. Wong, “High speed flow visualization of a closed loop pulsating heat pipe,” *Int. J. Heat Mass Transfer*, vol. 48, pp. 3338–3351, 2005. DOI:10.1016/j.ijheatmasstransfer.2005.02.034.
[27] E. Sedighi, A. Amarloo, and B. Shafii, “Numerical and experimental investigation of flat-plate pulsating heat pipes with extra branches in the evaporator section,” *Int. J. Heat Mass Transfer*, vol. 126, pp. 431–441, 2018. DOI:10.1016/j.ijheatmasstransfer.2018.05.047.
[28] Q. Sun, J. Qu, J. Yuan, and H. Wang, “Start-up characteristics of MEMS-based micro oscillating heat pipe with and without bubble nucleation,” *Int. J. Heat Mass Transfer*, vol. 122, pp. 515–528, 2018. DOI:10.1016/j.ijheatmasstransfer.2018.02.003.
[29] K. Mehta and N. Mehta, “Development of flat plate oscillating heat pipe as a heat transfer device,” *Front Heat Pipes (FHP)*, vol. 7, pp. 1–7, 2016. DOI:10.5098/fhp.7.6.
[30] M. Mohammadi, M. Mohammadi, A. R. Ghahremani, M. B. Shafii, and N. Mohammadi, “Experimental investigation of thermal resistance of a ferrofluidic closed-loop pulsating heat pipe,” *Heat Transfer Eng.*, vol. 35, pp. 25–33, 2014. DOI:10.1080/01457632.2013.810086.
[31] K. A. Stevens, S. M. Smith, and B. S. Taft, “Variation in oscillating heat pipe performance,” *Appl. Therm. Eng.*, vol. 149, pp. 987–995, 2019. DOI:10.1016/j.applthermaleng.2018.12.113.

[32] S. Khandekar, M. Schneider, P. Schafer, R. Kulenovic, and M. Groll, "Thermofluid dynamic study of flat-plate closed-loop pulsating heat pipes," *Microscale Thermophys. Eng.*, vol. 6, pp. 303–317, 2002. DOI:10.1080/10893950290098340.

[33] H. Yang, S. Khandekar, and M. Groll, "Operational characteristics of flat plate closed loop pulsating heat pipes," 13th International Heat Pipe Conference, Shanghai, China, 2004, pp. 291–297.

[34] W. Qu and B. Yang, "Performances of flat plate pulsating heat pipes," ASME 2009 Second International Conference on Micro/Nanoscale Heat and Mass Transfer, Shanghai, China, 2009, pp. 403–410.

[35] P. Cheng, S. Thompson, J. Boswell, and H. Ma, "An investigation of flat-plate oscillating heat pipes," *J. Electron. Packag.*, vol. 132, pp. 041009, 2010. DOI:10.1115/1.4002726.

[36] K. Chien, Y. Chen, Y. Lin, C. Wang, and K. Yang, "The experimental studies of flat-plate closed-loop pulsating heat pipes," The tenth international heat pipe symposium, Taipei, Taiwan, 2011, pp. 212–216.

[37] F. Lefèvre, *et al.*, "Flat plate heat pipes: from observations to the modeling of the capillary structure," *Front Heat Pipes (FHP)*, vol. 3, pp. 1–9, 2012. DOI:10.5098/fhp.v3.1.3001.

[38] M. P. Hoesing and G. J. Michna, "Integration of a pulsating heat pipe in a flat plate heat sink," ASME 2014 12th International Conference on Nanochannels, Microchannels, and Minichannels, Chicago, IL, 2014.

[39] F. Laun, H. Lu, and H. Ma, "An experimental investigation of an oscillating heat pipe heat spreader," *J. Therm. Sci. Eng. Appl.*, vol. 7, pp. 2100–2105, 2015. DOI:10.1115/1.4026815.

[40] T. Hao, X. Ma, Z. Lan, N. Li, and Y. Zhao, "Effects of superhydrophobic and superhydrophilic surfaces on heat transfer and oscillating motion of an oscillating heat pipe," *J. Heat Transfer*, vol. 136, pp. 082001, 2014. DOI:10.1115/1.4027390.

[41] S. M. Thompson, H. Lu, and H. Ma, "Thermal spreading with flat-plate oscillating heat pipes," *J. Thermophys Heat Transfer*, vol. 29, pp. 338–345, 2014. DOI:10.2514/1.T4168.

[42] V. Manno, *et al.*, "Thermal-hydraulic characterization of a flat plate pulsating heat pipe for automotive applications," *Interfacial Phenom. Heat Transf.*, vol. 3, 2015. DOI: 10.1615/InterfacPhenomHeatTransfer.2016013273.

[43] V. Ayel *et al.*, "Experimental study of a closed loop flat plate pulsating heat pipe under a varying gravity force," *Int. J. Therm. Sci.*, vol. 96, pp. 23–34, 2015. DOI: 10.1016/j.ijthermalsci.2015.04.010.

[44] F. Zhang, *et al.*, "Effect of hydrophilic nanostructured cupric oxide surfaces on the heat transport capability of a flat-plate oscillating heat pipe," *J. Heat Transfer*, vol. 138, pp. 062901, 2016. DOI:10.1115/1.4032608.

[45] J. Lee and S. J. Kim, "Effect of channel geometry on the operating limit of micro pulsating heat pipes," *Int. J. Heat Mass Transf.*, vol. 107, pp. 204–212, 2017. DOI:10.1016/j.ijheatmasstransfer.2016.11.036.

[46] D. S. Jang, J. S. Lee, J. H. Ahn, D. Kim, and Y. Kim, "Flow patterns and heat transfer characteristics of flat plate pulsating heat pipes with various asymmetric and aspect ratios of the channels," *Appl. Therm. Eng.*, vol. 114, pp. 211–220, 2017. DOI:10.1016/j.applthermaleng.2016.11.189.

[47] A. Yoon and S. J. Kim, "Characteristics of oscillating flow in a micro pulsating heat pipe: fundamental-mode oscillation," *Int. J. Heat Mass Transfer*, vol. 109, pp. 242–253, 2017. DOI:10.1016/j.ijheatmasstransfer.2017.02.003.

[48] M. Hoesing, "Integration of a pulsating heat pipe in a flat plate heat sink," *J. Undergraduate Res.*, vol. 12, pp. 4, 2014. openprairie.sdstate.edu/jur/vol12/iss1/4.

[49] D. Bastakoti, H. Zhang, D. Li, W. Cai, and F. Li. "An overview on the developing trend of pulsating heat pipe and its performance," *Appl. Therm. Eng.*, 2018. DOI: 10.1016/j.applthermaleng.2018.05.121.

[50] M. B. Shafii, A. Faghri, and Y. Zhang, "Thermal modeling of unlooped and looped pulsating heat pipes," *J. Heat Transfer*, vol. 123, pp. 1159–1172, 2001.

[51] H. Yang, S. Khandekar, and M. Groll, "Operational limit of closed loop pulsating heat pipes," *Appl. Therm. Eng.*, vol. 28, pp. 49–59, 2008.

[52] Q. Cai, C. Chen, and J. F. Asfia, "Operating characteristic investigations in pulsating heat pipe," *J. Heat Transfer*, vol. 128, pp. 1329–1334, 2006. DOI:10.1115/1.2349509.

[53] P. Charoensawan, S. Khandekar, M. Groll, and P. Terdtoon, "Closed loop pulsating heat pipes: part A: parametric experimental investigations," *Appl. Therm. Eng.*, vol. 23, pp. 2009–2020, 2003. DOI:10.1016/S1359-4311(03)00159-5.

[54] M. Saha, C. Feroz, F. Ahmed, and T. Mujib, "Thermal performance of an open loop closed end pulsating heat pipe," *Heat Mass Transfer*, vol. 48, pp. 259–265, 2012. DOI:10.1007/s00231-011-0882-9.

[55] J. Qu, H. Wu, and P. Cheng, "Start-up, heat transfer and flow characteristics of silicon-based micro pulsating heat pipes," *Int. J. Heat Mass Transf.*, vol. 55, pp. 6109–6120, 2012. DOI:10.1016/j.ijheatmasstransfer.2012.06.024.

[56] H. Ma. *Oscillating Heat Pipes*. Springer, New York, 2015.

[57] T. Hao, H. Ma, and X. Ma, "Heat transfer performance of polytetrafluoroethylene oscillating heat pipe with water, ethanol, and acetone as working fluids," *Int. J. Heat Mass Transfer*, vol. 131, pp. 109–120, 2019. DOI:10.1016/j.ijheatmasstransfer.2018.08.133.

[58] H. Wang, D. Yin, and H. Ma, "Heat transfer analysis of a liquid plug flowing in a tube," *Heat Transfer Res.*, vol. 48, pp. 757–769, 2017.

[59] T. Hao, X. Ma, and Z. Lan, "Effects of hydrophilic and hydrophobic surfaces on start-up performance of an oscillating heat pipe," *J. Heat Transfer*, vol. 140, pp. 012002, 2018.

[60] W. Wits, G. Groeneveld, and H. J. Van Gerner. "Experimental investigation of a flat-plate closed-loop pulsating heat pipe," *J. Heat Transfer*, 2018. DOI: 10.1115/1.4042367.
[61] J. Lim and S. J. Kim, "Fabrication and experimental evaluation of a polymer-based flexible pulsating heat pipe," *Energy Convers. Manage.*, vol. 156, pp. 358–364, 2018.
[62] Q. Liang, *et al.*, "Startup and transport characteristics of oscillating heat pipe using ionic liquids," *Int. Commun. Heat Mass Transfer*, vol. 94, pp. 1–13, 2018.
[63] J. Lee, Y. Joo, and S. J. Kim, "Effects of the number of turns and the inclination angle on the operating limit of micro pulsating heat pipes," *Int. J. Heat Mass Transfer*, vol. 124, pp. 1172–1180, 2018.
[64] W. Kim and S. J. Kim, "Effect of reentrant cavities on the thermal performance of a pulsating heat pipe," *Appl. Therm. Eng.*, vol. 133, pp. 61–69, 2018.
[65] A. Cecere, *et al.* "Experimental analysis of a flat plate pulsating heat pipe with self-rewetting fluids during a parabolic flight campaign," *Acta Astronaut.*, vol. 147, pp. 454–461, 2018.
[66] V. Ayel, *et al.*, "Visualization of flow patterns in closed loop flat plate pulsating heat pipe acting as hybrid thermosyphons under various gravity levels," *Heat Transfer Eng.*, pp. 1–11, 2018. DOI: 10.1080/01457632.2018.1426244.
[67] J. Qu, Q. Sun, H. Wang, D. Zhang, and J. Yuan, "Performance characteristics of flat-plate oscillating heat pipe with porous metal-foam wicks," *Int. J. Heat Mass Transfer*, vol. 137, pp. 20–30, 2019. DOI:10.1016/j.ijheatmasstransfer.2019.03.107.
[68] J. Lim and S. J. Kim, "Effect of a channel layout on the thermal performance of a flat plate micro pulsating heat pipe under the local heating condition," *Int. J. Heat Mass Transfer*, vol. 137, pp. 1232–1240, 2019. DOI:10.1016/j.ijheatmasstransfer.2019.03.121.
[69] S. Jun and S. J. Kim, "Experimental investigation on the thermodynamic state of vapor plugs in pulsating heat pipes," *Int. J. Heat Mass Transfer*, vol. 134, pp. 321–328, May. 2019. DOI: 10.1016/j.ijheatmasstransfer.2019.01.053.
[70] K. Mehta, P. Gamit, and A. Pandey, "Influence of working fluids on thermal performance of flat plate oscillating heat pipe," *Int. J. Res. Appl. Sci. Eng. Technol.*, vol. 7, pp. 399–403, 2019.
[71] X. Cui, Y. Zhu, Z. Li, and S. Shun, "Combination study of operation characteristics and heat transfer mechanism for pulsating heat pipe," *Appl. Therm. Eng.*, vol. 65, pp. 394–402, 2014.
[72] A. Yoon and S. J. Kim, "Experimental and theoretical studies on oscillation frequencies of liquid slugs in micro pulsating heat pipes," *Energy Convers. Manage.*, vol. 181, pp. 48–58, 2019. DOI:10.1016/j.enconman.2018.11.060.
[73] Q. Sun, J. Qu, J. Yuan, and Q. Wang, "Operational characteristics of an MEMS-based micro oscillating heat pipe," *Appl. Therm. Eng.*, vol. 124, pp. 1269–1278, 2017.
[74] M. Vassilev, Y. Avenas, C. Schaeffer, J.-L. Schanen, and J. Schulz-Harder, "Experimental study of a pulsating heat pipe with combined circular and square section channels," 2007 IEEE Industry Applications Annual Meeting, New Orleans, LA, 2007, pp. 1419–1425.